Invited paper

Semiconductor ultraviolet photodetectors

ANTONI ROGALSKI*[1] and MANIJEH RAZEGHI[2]

[1] Institute of Applied Physics, Military University of Technology, Warsaw, Poland
Center for Quantum Devices, Department of Electrical Engineering
and Computer Science Northwestern University, Evanston, Illinois, USA

This paper presents an overview of semiconductor ultraviolet (UV) photo--detectors that are currently available and associated technologies that are undergoing further development. At the beginning, the classification of UV detectors and general requirements imposed on these detectors are presented. Further consideration are restricted to modern semiconductor UV detectors, so the current state-of-the art of different types of semiconductor UV detectors is presented. Hitherto, the semiconductor UV detectors have been mainly fabricated using Si. Industries such as the aerospace, automotive, petroleum, and others have continuously provided the impetus pushing the development of fringe technologies which are tolerant of increasingly high temperatures and hostile environments. As a result, the main effort are currently directed to a new generation of UV detectors, fabricated from wide-band-gap semiconductors; between them the most promising are diamond and AlGaN. The latest progress in development of AlGaN UV detectors is finally described in detail.

1. Introduction

The issue of UV detectors is treated in several monographs and reviews. An extensive examination of various detector systems for both imaging and nonimaging applications is presented by Carruthers [1]. Timothy and Madden [2] have restricted their review to photon detectors that are currently available for use at ultraviolet and X-ray wavelengths. More information about the history of the development of UV detectors and their current status in astronomy can be found in excellent book entitled *Low light level detectors in astronomy* by Eccles, Sim and Tritton [3]. Another Timothy's review paper is devoted mainly to detectors for optical wavelengths [4], and a comparison of charge-coupled devices (CCDs) to other optical detectors is given by Janesick et al. [5]. The reviews of the present and future technological concepts currently being considered in astrophysics and astronomy are given by Welsh and Kaplan [6], Joseph [7], and by Ulmer et al. [8]. However, the UV detectors have also found terrestrial applications. They can detect UV emissions from flames in the presence of hot backgrounds (such as infrared emission from the hot bricks in a furnace). This provides an excellent flame on/off determination system for controlling the gas supply to large furnaces and boiler systems. Flame safeguard and fire control areas are

* corresponding author: Antoni Rogalski, Institute of Applied Physics, Military University of Technology, 2 Kaliskiego Str., PL-01-489 Warsaw, Poland.

just two of the various possible applications of the UV detectors.

In this paper we will first present the classification of UV detectors and general requirements imposed on these detectors. Further consideration will be restricted to modern semiconductor UV detectors, so the current state-of-the art of different types of semiconductor UV detectors will be presented. The main effort will be especially directed to a new generation of UV detectors. This generation of detectors is the product of five years of materials and device research, which resulted in the development of high quality GaN layers.

2. Classification of UV detectors

In general, UV detectors fall into two categories: photon detectors (also named photodetectors) and thermal detectors (see Fig. 1). In photon detectors the incident photons are absorbed within the material by interaction with electrons. The observed electrical signal results from the changed electronic energy distribution. The photon detectors measure the rate of arrival of quanta and show a selective wavelength dependence of the response per unit incident radiation power. In thermal detectors, the incident radiation is absorbed and raises the temperature of the material. The output signal is observed as a change in some temperature-dependent property of the material. In pyroelectric detectors a change in the internal electrical polarization is measured, whereas in the case of bolometers a change in the electrical resistance is measured. The thermal effects are generally wavelength-independent since the radiation can be absorbed in a "black" surface coating. Because of greater sensitivity, photon detectors are more commonly utilized at UV wavelengths. Thermal detectors, however, are sometimes employed at UV wavelengths as absolute radiometric standards.

UV photon detectors have traditionally been devoted into two distinct classes; namely, photographic and photoelectric. Photographic emulsion has the great advantage of an image-storing capability and can thus record a large amount of data in a single exposure. However, photographic emulsion has a number of limitations: the sensitivity is considerably lower that that of a photoelectric detector, the dynamic range is limited, the response is not a linear function of the incident photon flux at a specific wavelength, and emulsion is sensitive to a very wide energy range.

Photoelectric detectors, on the other hand, are more sensitive, have a greater stability of response and provide better linearity characteristics. In the last decade considerable progress in the image-recording capability of photoelectronic devices has been observed. Recently developed photovoltaic array detectors and photoemissive array, for the first time, combine the sensitivity and radiometric stability of a photomultiplier with a high-resolution imaging capability.

In the most commonly employed photoemissive UV detectors, the photon is allowed to impact a solid surface realizing a photoelectron into the vacuum environment [Fig. 2(a)]. Applying a voltage between the photocathode surface and a po-

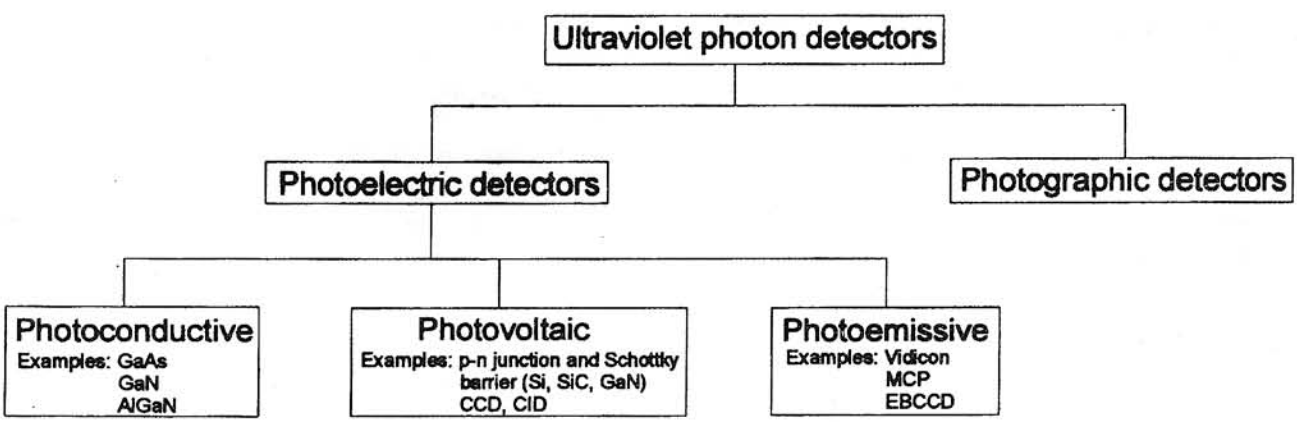

Fig. 1. Classification of ultraviolet detectors.

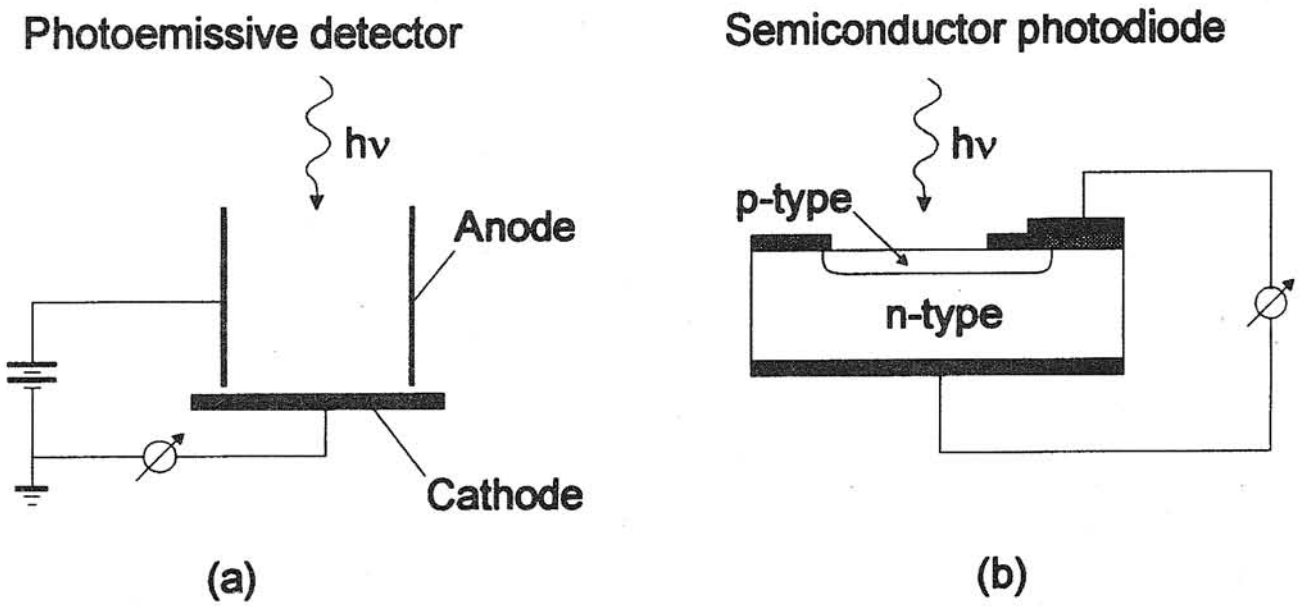

Fig. 2. Principle of operation of photoemissive (a) and semiconductor detectors (b).

sitively-biased anode causes a photoelectron current to flow in proportion to the intensity of the incident radiation. Since these detectors make use of the external photoelectric effect, the wavelength range of sensitivity is defined primarily by the work function of the surface material. Photocathode materials such as SbKCs and CsTe exhibit maximum sensitivity in the range from 400 to 235 nm, respectively, making them well suited to UV applications.

In the semiconductor detectors, the photons are absorbed in the bulk of the semiconductor material, producing electron-hole pairs which are separated by an electrical field. These detectors make use of the internal photoelectric effect where the energy of the photons is large enough to raise the electrons into the conduction band of the semiconductor material. In the case of photovoltaic detectors, the electron-hole pairs are separated by the electrical field of p-n junctions, Schottky barrier or MIS capacitors, which leads to an external photocurrent proportional to the number of detected photons [Fig. 2(b)].

In the photoemissive detectors, the primary photoelectron can be multiplied by the process of secondary emission to produce a large cloud of electrons. The occurrence of a single photoelectron event then can be detected either directly with conventional electronic circuits or by accelerating the electron cloud to high energy and allowing it to impact a phosphor screen. The emitted pulse of visible-light photons can then be viewed directly, or detected and recorded by additional photosensitive systems. Detectors operated in this pulse-counting mode can provide the ultimate level of sensitivity set by the quantum efficiency of the photocathode. The complexities of photomultiplier tube (amplification in a vacuum tube, high voltages required, large and fragile tubes are sensitive to magnetic field, expensive) limit their applications, especially for those requiring small devices, consuming small power.

Table I. Comparison of photoemissive and semiconductor UV detectors

Type	Advantages	Disadvantages
Photoemissive detectors	easy to operate, high sensitivity solar blind	low quantum efficiency, strong spectral dependence of responsivity, sensitiveness to surface contaminations
Semiconductor detectors	broad spectral responsivity, excellent linearity, high quantum efficiency, high dynamic range of operation, large-format image arrays	induced aging effects

The importance of UV semiconductor detectors has resulted in the recent meteoric expansion of the semiconductor industry, and second, the continuing emphasis on the development of low-light-level imaging systems for military and civilian surveillance applications. These detectors should:

- not be sensitive to light at optical wavelengths (commonly referred to as being solar blind),
- have high quantum efficiency,
- have a high dynamic range of operation,
- have low backgrounds since noise arising from the background often dominates in faint UV observations.

Multiplying the number of primary charge carriers is generally not possible in semiconductor detectors (although this deficiency may be offset by the very high internal quantum efficiency of the semiconductor material). These detectors are thus less sensitive at the lowest signal levels than the photoemissive detectors operating in pulse-counting mode. However, the semiconductor detectors have the ability to store charge and integrate the detected signal for significant periods of time. In recent time, there has been much development of charge couple device (CCD) detectors for use in the UV spectral ranges [5, 9 – 12]. On the contrary, for visible spectral range, the use of Si CCDs in the UV region is not yet well established because of the many problems connected with the interaction of UV radiation with the materials typically used in silicon technology. However, a new class of video-rate imagers based on thinned, back-illuminated CCDs is available at present to replace conventional image intensifiers [12].

3. Semiconductor materials used for UV detectors

Ultraviolet semiconductor photodetectors work in three fundamental modes:

- photoconductive detectors,
- photodiode p-n junctions, and
- Schottky barrier detectors.

The basic theories of photoconductors, p-n junctions and Schottky barriers are presented in Ref. 13.

Different semiconductor compounds have been used to fabricate photodetectors with spectral responses in the UV region. Figure 3 shows the spectral detectivity of optical detectors responding in the 0.1 to 1.2 μm region. Note that detectivity is not D*, but rather reciprocal of NEP for a 1 Hz bandwidth. This figure of merit is employed to include photomultipliers whose noise does not in all cases depend upon the square root of the photocathode area.

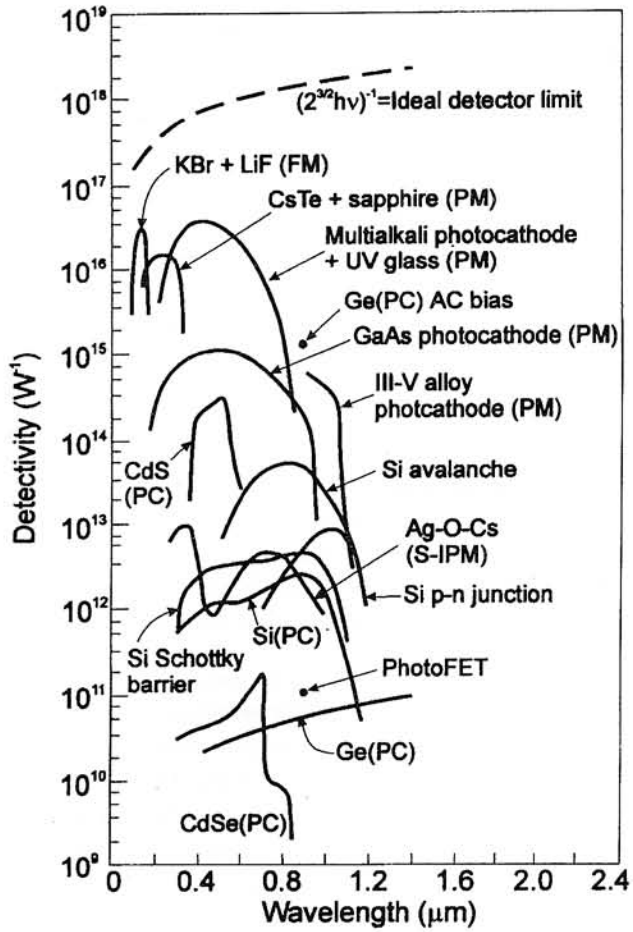

Fig. 3. Detectivty vs wavelength values of 0.1-1.2 μm photodetectors. PC indicates a photoconductive detector and PM indicates a photomultiplier(after Ref. 14)

Historically, the development of a high quantum efficiency semiconductor detectors in the whole UV range has been hampered by the extremely strong absorption and strong radiation induced aging effects in most of the semiconductor materials. It is especially visible in the case of silicon, which due to mature technology, is the most

popular semiconductor material used for fabrication of UV detectors. For this semiconductor the photon penetration depth ranged from less than 10 nm in the near UV and mid UV to 100 μm for 10-keV X-rays [1].

The modern semiconductor UV detectors are mainly fabricated using Si. These devices offer the advantages inherent in a small (in comparison with photomultiplier tube), solid state device, requiring only moderate voltages. Disadvantage of this approach include the fact that Si is an indirect bandgap material, so that quantum efficiency is low, and that the peak sensitivity is around 700 nm, so that external filtering is needed to block out the visible and infrared light, this adding both to the expense and volume of the detector assembly. What is needed is a detector which combines – the compactness, low voltage operation of the Si photodiode, with the solar blind capabilities of the photomultiplier tube.

Many of applications for UV detection involve hostile environments such as *in situ* combustion monitoring and satellite-based missile plume detection, where the ruggedness of active UV detector material is an important advantage. Other applications capitalize on the sensitivity of wide-band-gap semiconductor detectors, such as air quality monitoring, gas sensing, and personal UV exposure dosimetry. Industries such as the aerospace, automotive, petroleum, and others have continuously provided the impetus pushing the development of fringe technologies which are tolerant of increasingly high temperatures and hostile environments. In the field of optical devices, several trends are pushing research into new materials. The next generation of UV detectors are those based on wide bandgap semiconductors (E_g > 3.0 eV). Considering the relatively advanced stage of SiC development, it appears that most high-temperature, high-power electronic devices will be fabricated from that material. The wide bandgap energy permits also the fabrication of SiC UV detectors. A technological progress in fabrication of materials based on the III-V nitrides together with their inherent favorable properties, make III-V nitrides the most promising semiconductor materials for application in the UV wavelength range [15, 16]. III-V nitride devices will be capable of improved high-power and -temperature operation due to their large band gaps.

GaN has many advantages over SiC for applications, but lags in development. While its thermal conductivity, thermal stability, chemical inertness, breakdown fields, and band gap are all roughly comparable to SiC, its optoelectronic properties will be superior. GaN has a direct band gap, so momentum-conserving transitions connect states having the same k values. Therefore, GaN is one of the most promising materials for light-emitting devices in the blue, violet and ultraviolet spectral regions. Because of the wide bandgap of GaN (E_g = 3.4 eV) there is no responsivity to infrared radiation (long wavelength cutoff occurs at 365 nm) which is important in many applications whenever it is desirable to detect UV in a visible and infrared background. It should be expected that GaN radiation resistance is superior to SiC. Initial results indicate that ohmic contacts to GaN will be superior to those possible with SiC. Finally, the ease with which heterostructures can be formed with AlN and InN alloys is a great advantage for more complex device structures.

The wurtzite polytypes of GaN, AlN, and InN form continuous alloy systems whose direct band gaps range from 1.9 eV for InN, to 3.4 eV for GaN, to 6.2 eV for AlN. Thus, the III-V nitrides could potentially be fabricated into optical devices which are active at wavelengths ranging from the red well into the UV. Table 2 compares relevant material properties of SiC and GaN with Si and GaAs, the two most popular semiconductor device technologies, and GaP and diamond, two other contenders for high-temperature operations. Diamond has long been recognized as a promising material for fabricating robust, solar-blind radiation detectors. However, due to technological limitation, diamond is still potential material for future technologies [17].

4. Si UV photodiodes

Silicon photodiodes originally designed for the visible spectral range, can be also used in the UV region. Arrays of silicon photodiodes are fabricated by a number of manufacturers, e.g. the most commonly used arrays for astronomical spectroscopy are fabricated by EG and Reticon [18]. Building a silicon photodiode with a high ultraviolet quantum efficiency has not been the pro-

Table II. Comparison of important semiconductor properties for high-temperature electronics (after Refs. 15 and 16)

Parameter	Si	GaAs	GaP	3C-SiC (6H-SiC)	GaN	Diamond
Lattice parameters (Å)	a = 5.4301	a = 5.6533		a = 4.36 (a = 3.08) (c = 15.12)	a = 3.189 c = 5.185	
Band gap (eV) at 300 K	1.1	1.4	2.3	2.2 (2.9)	3.39	5.5
Coefficient of thermal expansion ($10^{-6}K^{-1}$)	3.59	6.0		(4.2) (4.68)	5.59 3.17	
Maximum operating temperature (K)	600?	760?	1250?	1200 (1580)		1400?
Melting point (K)	1690	1510	1740	Sublimes >2100		Phase changes
Physical stability	Good	Fair	Fair	Excellent	Good	Very good
Electron mobility (cm^2/Vs) at 300 K	1400	8500	350	1000 (600)	900	2200
Hole mobility (cm^2/Vs) at 300 K	600	400	100	40	150?	1600
Breakdown voltage (10^6 V/cm)	0.3	0.4	–	4	5?	10
Thermal conductivity (W/cm)	1.5	0.5	0.8	5	1.3	20
Saturation electron drift velocity (10^7 cm/s)	1	2	–	2	2.7	2
Static dielectric constant	11.8	12.8	11.1	9.7	9	5.5

blem. The problem has been to maintain that high quantum efficiency under ultraviolet irradiation and over a period of years.

Two types of silicon UV detectors are fabricated:

- diffused photodiode,
- Schottky barrier photodiode.

The majority of the oldest types of silicon photodiodes had a dead region at their surface, so carriers generated by UV photons were lost in this region before they could be collected by the p-n junction, leading to a loss of quantum efficiency. Even if a photodiode had 100% internal quantum efficiency, a thick silicon dioxide layer on the diode surface would reduce the quantum efficiency in the 400 Å to 1200 Å region drastically.

To overcome above mentioned difficulties, it has been proposed and demonstrated that natural inversion layer photodiodes [19] should have an internal short-wavelength quantum efficiency of 100% due to the nature of the built-in field associated with a strongly inverted layer at the oxide-silicon interface. Figure 4(a) shows a schematic diagram of this photodiode. The inversion layer is contacted via the n^+-diffusion by means of the inner metal ring. The outer metal ring contacts the p^+-guarding and thereby the p-substrate. The substrate can also be connected via the p^+-diffusion on the back side. The intrinsic fixed positive charge within the SiO_2 causes the p-type substrate to undergo inversion, and thus induces a very thin n-type region adjacent to the SiO_2/Si interface, and forms the required p-n junction. Since the junction creation process results in a built-in field which is optimum for removing minority carriers from the oxide-silicon interface, these devices are less prone to recombination and trapping effects, and thus higher UV quantum efficiency can be achieved than in the case of diffused junction photodiodes.

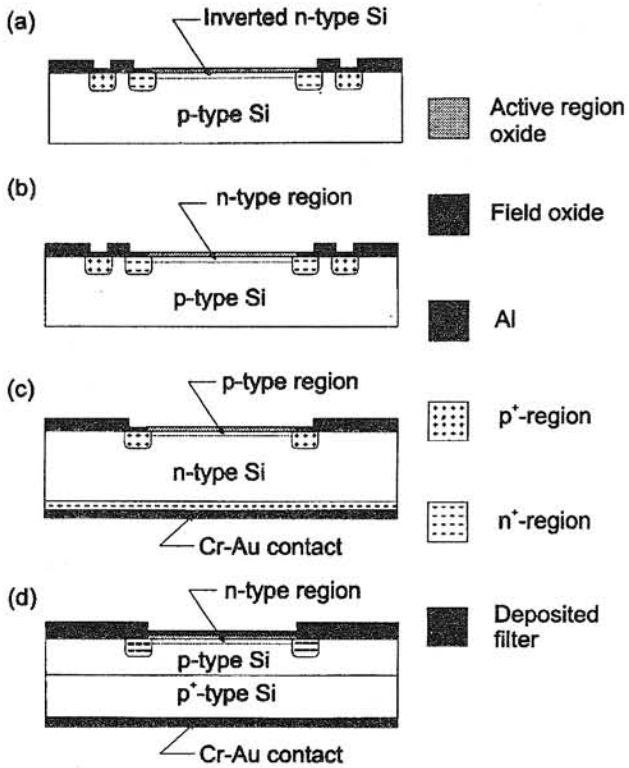

Fig. 4. Schematic diagram of the silicon UV photodiodes: (a) inversion layer type; (b) phosphorus diffused type (n on p); (c) boron-diffused type (p on n) (after Ref. 20), and (d) optically filtered arsenic diffused (n on p) (after Ref. 21).

Figure 5 shows spectral dependence of quantum efficiency of UDT standard UV 100 inversion layer photodiodes which had 1200 Å antireflection layers of oxide. The absence of any dead region at the front surface of these diodes has been verified by internal quantum efficiency measurements in the 250–500 nm spectral range. These diodes are also almost dead below 1200 Å because of the thick silicon oxide antireflecting coating on the front surface. Because the inversion layer charge which causes the semiconductors surface inversion is situated within the first 100 Å of silicon oxide from the semiconductor surface, any efforts to extend the diodes response below 1200 Å by reducing the silicon oxide coating to a few tens of Angstroms is undesirable.

Instabilities were also encountered with this type of photodiode. Inversion layer diodes have a low linearity due to the inherently high sheet resistance of an inverted semiconductor layer. Moreover, it appears, that the fixed oxide charge that induces the inversion layer in the diode was neutralized as a result of UV irradiation [20]. Since the inversion layer charge decreases with decreasing oxide charge, the diode inversion layer resistance, which is in series with the diode, would increase. Thus the threshold value of forward bias needed to cause a nonlinearity could be dropped across the increased series resistance by a small value of photocurrent, resulting in a loss of linearity range.

The best quality Si photodiodes for UV applications have been developed by Korde and co-workers [20, 22–24]. They used different methods of junction fabrication, but the better results have been obtained using defect-free arsenic [23] and phosphorus [20, 24] diffusions.

Figure 4(b) is a schematic diagram of diffused type Si photodiode. The starting material was a float-zone, <111> oriented, p-type, 100 Ωcm. After the p^+ channel stop and n^+ guard ring were formed by selective boron and phosphorus diffusions, respectively, arsenic was predeposited in the active area of the device using a planar arsenic source. The arsenosilicate glass formed during the predeposition was etched in 10% hydrofluoric acid and the final passivating Si_2O anti-reflection coating with a thickness of about 600 Å was grown in dry oxygen. A standard photolithographic process was used to open windows at the desired locations in the diffused regions, and aluminum was vacuum evaporated on these windows for ohmic contacts.

Since UV radiation is absorbed in the first few hundred nanometers of silicon, the doped diffusions were kept shallow to minimize the possibility of recombination between the oxide-silicon interface and the junction. Low temperature dopant deposition and drive-in were adopted to get a shallow junction, about 0.2 μm.

It appears that n-type impurities such as phosphorus and arsenic tend to pile up in the silicon during the oxide growth, creating a built-in electric field near the oxide-silicon interface, which eliminates interface recombination [25, 26]. So a high minority carrier lifetime in the diffused region results in 100% internal quantum efficiency.

As a possible causes of instability of quantum efficiency of silicon UV photodiodes, we can

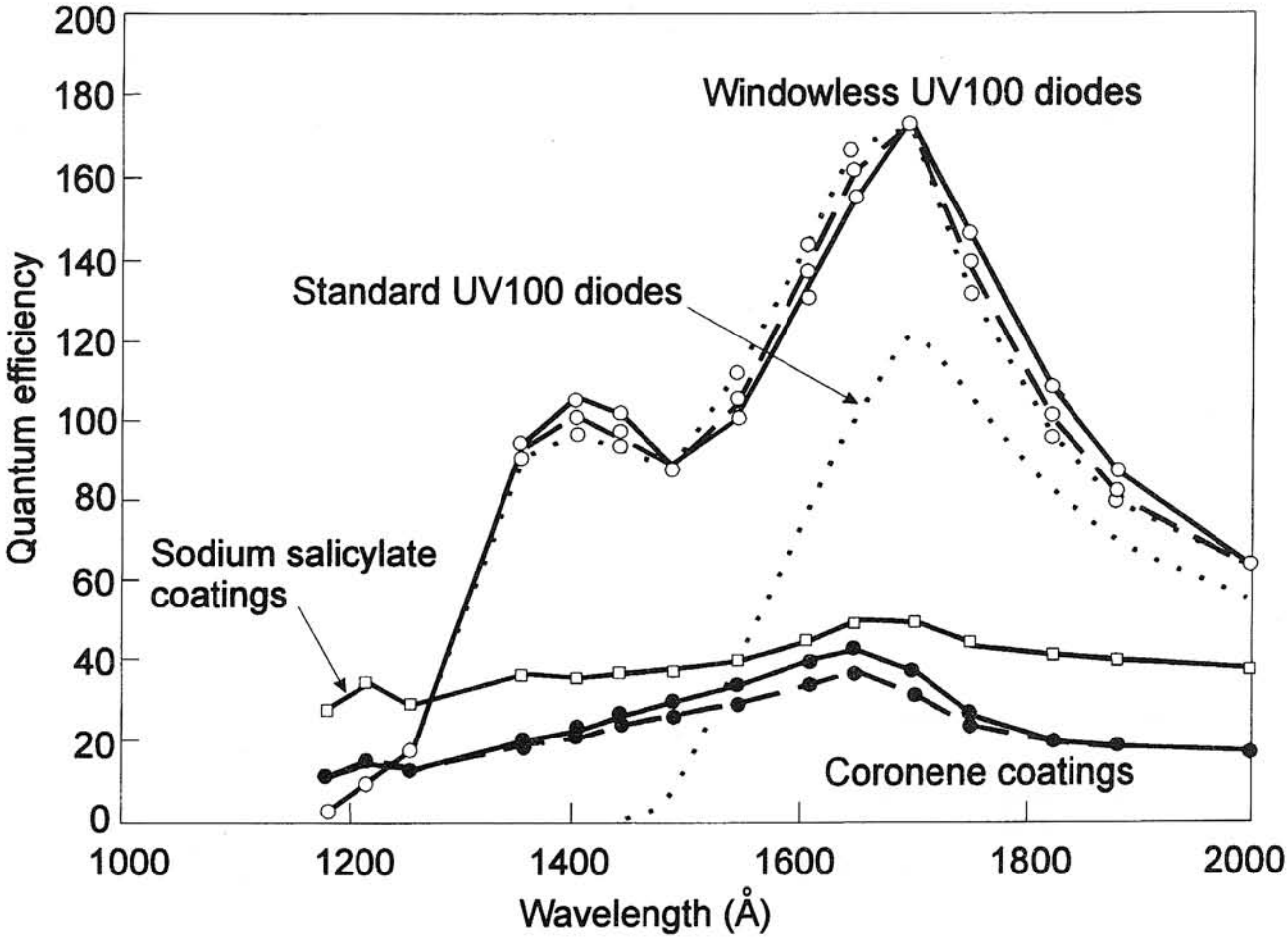

Fig. 5. Quantum efficiency of inversion layer silicon photodiodes (UDT standard UV 100 photodiodes) compared to the efficiency of typical fluorescing coatings (after Ref. 22).

distinguish [20]: unsatisfactory silicon-oxide interfaces, latent recombination centers in the diffused layers and moisture absorption by the device. Meticulous care as described in Ref. 20 is necessary during the fabrication of devices. A dry, clean oxide process during the growth of the final antireflection coating is essential to achieved stability against UV exposure.

N-on p photodiodes are inherently more stable than the commonly used boron-diffused devices based on n-type silicon. Boron migrates from the silicon surface into the oxide during the final thermal oxidation step. The resulting acceptor profile, which is depleted in the vicinity of the oxide-silicon interface, creates a built-in electric field perpendicular to the interface, directed toward the bulk. The resulting electric field attracts the photogenerated minority carriers (electrons) created in the diffused region towards the oxide-silicon interface, greatly enhancing the carrier loss due to interface recombination.

Further improvement in the fabrication of Si UV photodiodes has been achieved by reduction of the silicon dioxide layer to a thickness between 40 and 80 Å [22, 24]. The thinner oxide should lead to photodiodes with higher quantum efficiency stability because of the smaller volume available for generation of electron-hole traps which are invariably caused by the diode exposure to humidity and UV radiation. Production of the electron-hole traps in the passivating silicon dioxide layer is one of the major causes for quantum efficiency changes in silicon photodiodes.

One significant shortcoming of Si photodiodes for UV applications is the inherent broadband response extending from x-rays to the near infra-

red. The addition of a thin film of a suitable filtering material to the source of such a photodiode [see Fig. 4(d)] can accomplish the restriction of the sensitivity of the silicon to a much narrower band, or bands, in the UV [21].

5. SiC UV detectors

The inherent material properties of the 6H polytype of SiC are very attractive for UV applications. In comparison with Si (see Table 2), SiC is characterized by a higher breakdown field that permits much smaller drift regions (i.e., much lower drift region resistances), a higher thermal conductivity that enables superior heat dissipation, and a wide band-gap energy (2.9 eV) that permits higher junction operating temperature.

The earlier published research on 6H-SiC UV photodiodes utilized diffusion of Al into n-type substrates [27]. The diffusion process at temperatures of about 2000°C led to a structural decomposition of surface layers. This process resulted in high-leakage devices with low quantum efficiency. Glassow et al [28] improved upon this initial design by utilizing N implantation to form a very shallow (0.05 μm) n^+-p junction in a 5 μm p-type epitaxial layer, grown on a p-type substrate. Furnace annealing and rapid isothermal annealing (RIA) were employed to activate the implanted nitrogen. Further improvement has been achieved using commercial 6H SiC wafers, 1 inch in diameter, on which a p-n junction was grown epitaxially [29]. A heavily N-doped n-type epitaxial layer of 0.2 or 0.3 μm thick was utilized to form an n^+-p junction. The concentrations of impurities was 5 to 8 x 10^{17} cm^{-3} in p-type epitaxial layers, and 5 to 10 x 10^{18} cm^{-3} in n^+ cap layer. By thinning the top n^+ layer outside of the mesa contact, a responsivity of 50 mA/W was achieved at 200 nm. The diffusion length of electrons in the p-type layer was varied between 1.4 to 2.2 μm, and was smaller than the estimate of 3 μm given in Ref. 28.

Edmond and co-workers [30] have demonstrated the best quality 6H-SiC UV photodiodes. Wafers of n- and p-type 6H-SiC with typical resistivities in the range of 0.02–0.04 and 1–10 Ωcm, respectively, were used as substrates for epitaxial growth. An epitaxial junction was produced by first growing a predominantly Al-doped p-type layer followed by a predominantly N-doped n-type layer on a p-type substrate. The doping in the background layer was controlled between (1–5) x 10^{16} cm^{-3} with a thickness of ~3 μm. The n-type layer was heavily doped to ~10^{19} cm^{-3}. All devices were fabricated using a mesa geometry. The junctions were passivated with thermally grown SiO_2. Ohmic contact materials for the p-type side and n-type side were sintered Al and Ni, respectively.

The photodiode with square active junction with an area of 0.04 cm^2 has demonstrated extremely small dark currents, as little as 10^{-11} A at − 1 V at 473 K. At the highest voltage measured, − 10 V, the dark current density increased from ~10^{-9} to ~3 x 10^{-8} A/cm^2 when increasing the temperatures from 473 K to 623 K. Figure 6 shows the dark current density at − 10 V as a function of temperature together with previously reported data for comparison purposes. As shown, the devices reported by Edmond and co-workers [30] exhibit orders of magnitude lower leakage current than any other published data in 6H-SiC.

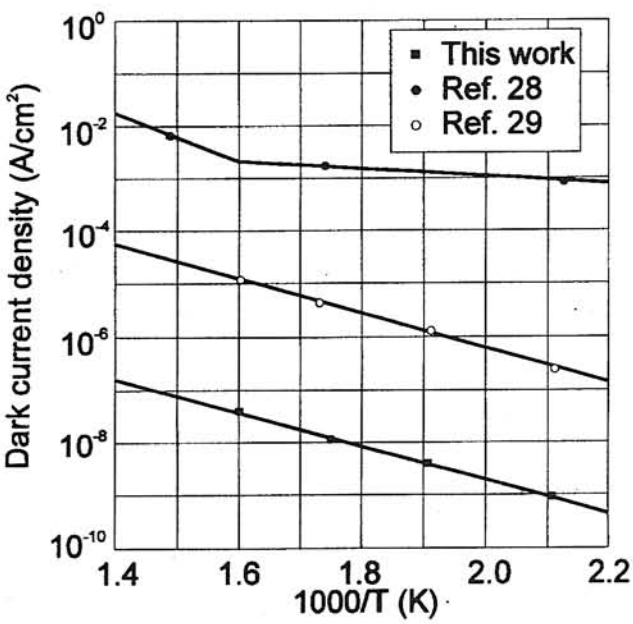

Fig. 6. Dark current density versus inverse temperature for 6H-SiC photodiodes (after Ref. 30).

The same devices exhibited near unity peak responsivities between 268 and 299 nm in tem-

perature range between 223 K and 623 K (see Fig 7). The responsivity of the photodiode at a higher temperature shifts to longer wavelengths because of bandgap narrowing. The indirect bandgap decreases from ~3.03 eV at 223 K to ~2.88 eV at 623 K, corresponding to a rate of 3.8×10^{-4} eV/K [28].

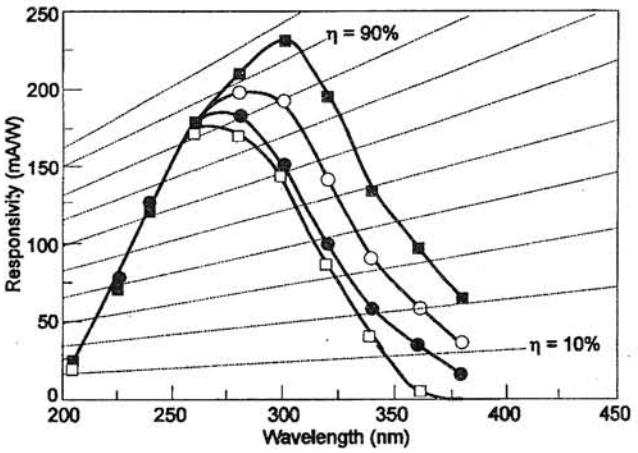

Fig. 7. Temperature-dependent responsivity of a SiC photodiode. The temperature tested were: (□) 223 K, (◆) 300 K, (o) 498 K and (■) 623 K (after Ref. 30).

Recently, Caputo et al. [31] have described large area p-i-n structures made of hydrogenerated amorphous silicon (a-Si:H) and silicon carbide (a-SiC:H) on glass substrate. An a-Si:H n-doped layer was first deposited on the transparent conductive SnO_2 film. Then the intrinsic a-SiC:H layer and the thin p-doped a-SiC:H layer were grown. On the top of the semiconducting structure, an aluminium 1 μm thick film was evaporated and photolitographically etched. At room temperature the detectors exhibit values of quantum efficiency of 20% at λ = 187 nm, and are transparent to the visible radiation.

Frojdh et al. [32, 33] have fabricated finger shaped Schottky photodiodes by evaporating Ti on substrates with different n-type and p-type doping levels. The starting material was 6H-SiC wafers with an epitaxial layer. The doping concentrations of the epitaxial layers have been changed between 10^{15} to 10^{18} cm^{-3}. As a barrier, titanium with resulting layer thickness 200 nm was evaporated on the wafers using an electron gun evaporator. A standard lift-off procedure was used to remove excess metal. A back contact was made by evaporation of 500 nm of Al on the back side of the wafer. Most of the Schottky barriers showed good rectifying behaviour with an ideality factor generally below 1.2. The best results were obtained for diodes on the p-type material for which the reverse leakage current at - 10 V was below 1 pA and for a reverse voltage of up to - 70 V the leakage current remained below 500 pA.

Generally, the p-type material shows a much higher photoresponse than the n-type material. This can be explained by two effects:

- the built in voltage in the p-type material is much higher (about factor of 2) than the built in voltage in the n-type material,
- the diffusion length of electrons is much larger than the diffusion length of holes.

6. III-V nitrides as the materials for UV detectors

The III-N nitrides are excellent materials to cover important technologically band, which occurs in the 240–280 nm range (~4.75 eV) where absorption by ozone makes the earth's atmosphere nearly opaque. Space communications in this band would be secure from earth, although vulnerable to satellite surveillance. On the earth, shielded by the suns radiation, imaging arrays operating in this band would provide extremely sensitive surveillance of objects coming up out of the atmosphere. Due to their wide band gap, the III-V nitrides are expected to exhibit superior radiation hardness characteristics compared to Si. GaN is by far the best-studied III-V nitride semiconductor.

The main obstacle in the development of the nitride UV photodetectors was significant difficulties in obtaining high-quality material. GaN has high n-type background carrier concentration resulting from native defects commonly thought to be nitrogen vacancies. In films having relatively small background electron concentrations, p-type doping is difficult to achieve. In the past several years much progress was made in developing modern epitaxial growth material. The room temperature background electron concentration of GaN films has been considerably reduced and p-type material has been reported. At present the

MOCVD grown GaN layers with the AlN buffer layer have n-type conductivity with an electron concentration of about 10^{15} cm^3 at room temperature and the electron mobility of about 500 cm^2/Vs [34]. Mg-doped p-type layers have hole concentrations above 10^{17} cm^3 and hole mobilities of 10–50 cm^2/Vs at room temperature [34, 35].

6.1. Photoconductive detectors

The first high quality GaN photoconductive detectors were fabricated by Khan et al. [36]. The active region of detector was a 0.8 μm-thick epitaxial layer of insulating GaN deposited over a 0.1-μm-thick AlN buffer layer using MOCVD over basal-plane sapphire substrates. Interdigitated, electrical, 5000-Å-thick, gold contacts were fabricated on the epilayers for the photoconductive response measurements. The interdigitated electrodes were 3 μm wide, 1 mm long, and had a 10 μm spacing. Figure 8 shows the spectral responsivity of GaN photoconductive detectors. It reaches its maximum value at 365 nm and then remains nearly constant down to 200 nm. The peak responsivity is about 1000 A/W, and the estimated gain/quantum efficiency product for the detectors is 4.8×10^3. The response of GaN detectors is linear over five orders of incident radiation power. The detector response time is about 1 ms.

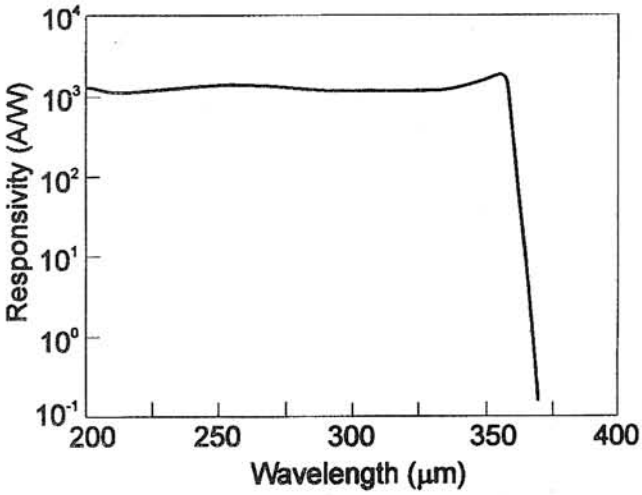

Fig. 8. Spectral responsivity for a GaN photoconductive detector (after Ref. 35).

Huang at al. [37] have reported the first 1x16 GaN linear array using a metal-semiconductor-metal structure and a conventional lift-off technique. Semi-insulating undoped GaN materials were grown by MOCVD at 1100°C. Each detector element contains 20 fingers on each side. These fingers are 2 μm wide, 500 μm long and are spaced 4 μm apart. The element and array are shown in Fig. 9. The ohmic contacts were made by evaporating 20 nm Ti, 30 nm Al followed by 120 nm Au, and annealing at 450°C for 5 min in an N_2 environment. The dark current for this array at 10 V is only 100 pA. The highest responsivity at 360 nm was $\approx$ 3250 Å/W and more than three orders of magnitude difference in responsivity between the UV region and the visible region was observed. Moreover, it has been found that arrays made from materials grown using a higher NH_3 flow rate showed better response time. The best detector, made from the sample grown under an NH_3 flow rate of 2200 cc/m, showed a turn-on time of 0.3 ms, and turn-off time of 0.6 ms.

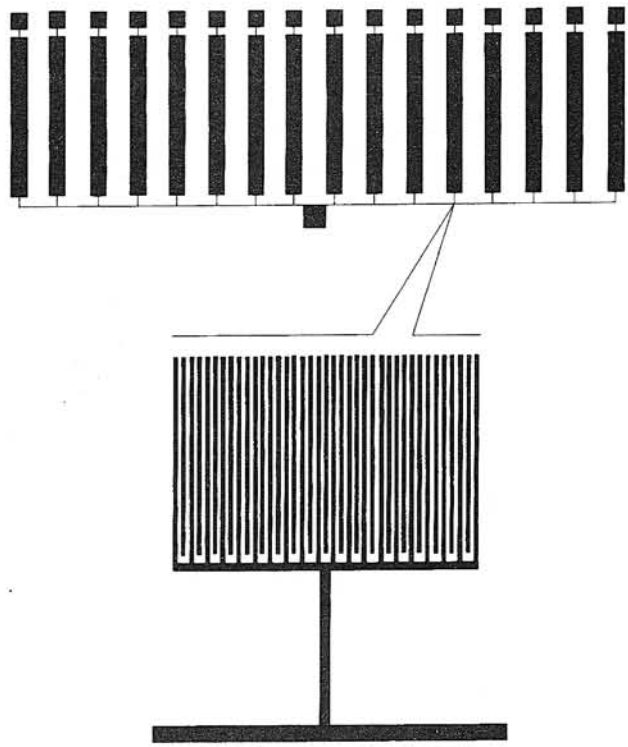

Fig. 9. Structure of GaN linear array (after Ref. 37).

The kinetic photoresponse of GaN samples has been reported in several papers [38–42]. P-type and n-type samples exhibit photoconductivity re-

sponses at photon energy far below the band-gap energy. It may be largely related to the deep tail states created by the high growth temperature, the large stress arising from the lattice mismatch to the substrate, impurity incorporation, and impurity compensation. Photocurrent decay of p-type GaN:Mg layers on Si substrates for a pulsed input show a hyperbolic type response [39]. It is hypothesized that holes are captured at either compensated Mg deep acceptor sites or Mg-related trap/recombination centers, resulting in a greatly prolonged electron free carrier lifetime. Instead, the photoconductivity decay of undoped n-type GaN films is characterized by an initial exponential decay followed by a quasi-law decay for decades of time longer than 1 μs [42]. The decay rate is insensitive to the electron concentration and is slightly temperature dependent. The minority carrier relaxation in n-type GaN is controlled by trapping at gap states. The trapped holes most probably dissipate through thermal excitation to the valence band followed by direct recombination and through tunneling to the defect centers that give rise to the yellow luminescence. The photoconductivity decay of n-type GaN films is very different from that controlled by recombination through dislocations.

Kung et al. [38] have studied the kinetics of the photoconductivity of n-type GaN photoconductive detectors by the measurements of the frequency dependent photoresponse and photoconductivity decay. Strongly sub-linear response and excitation-dependent response time have been observed even at relatively low excitation levels. This can be attributed to the redistribution of the charge carriers with increased excitation level. Consequence of this effect is decreasing of the photoconductive gain with increasing in UV intensity, what has been recently observed by Goldenberg et al. [43] (see Fig. 10).

The observed kinetics of photoresponse has important consequences for practical applica-

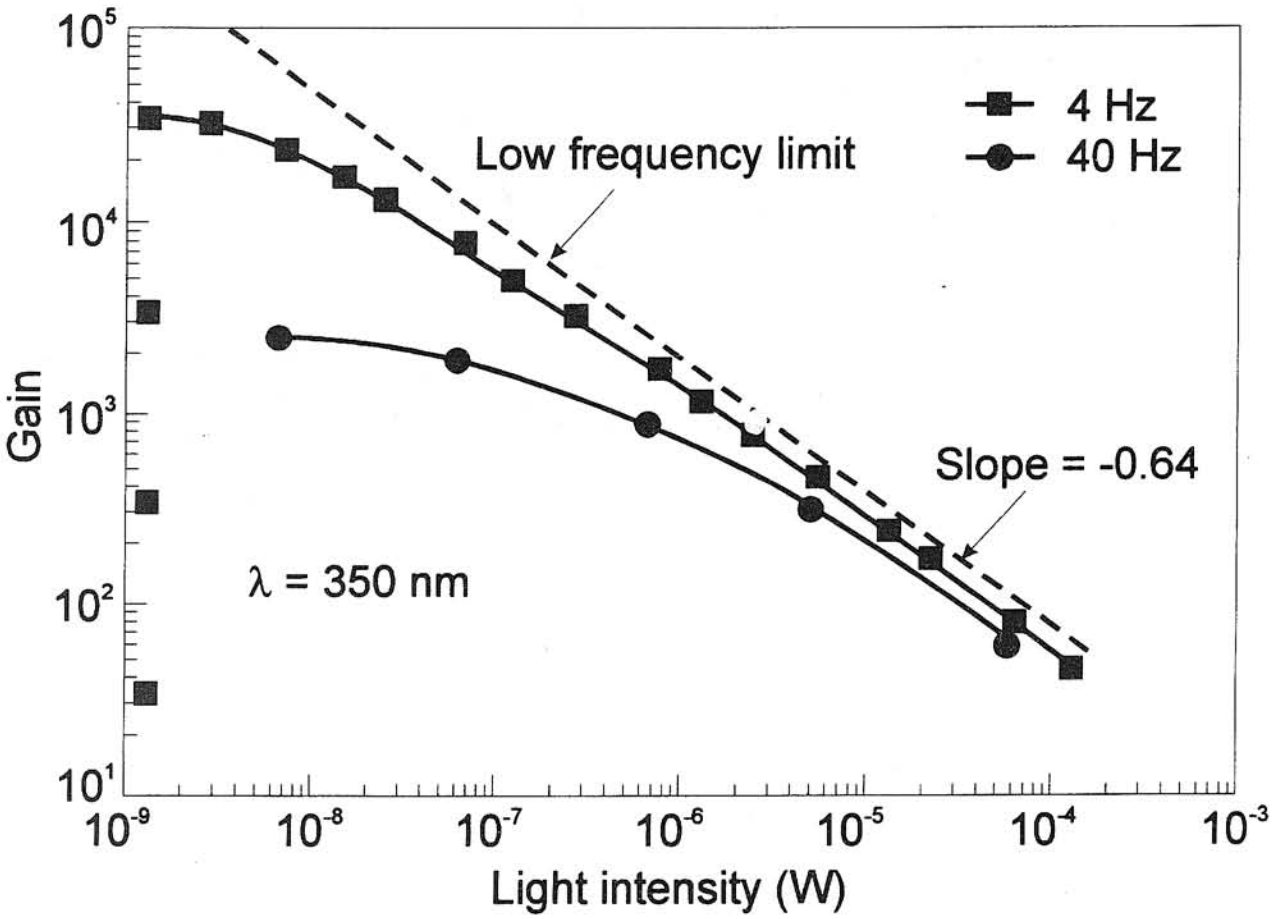

Fig. 10. The variation of photoconductive gain with intensity of light at 350 nm (after Ref. 37).

tions. The measured lifetimes are too long for many applications resulting in the frequency dependent responsivity and non-linear response. This can be changed in a number of ways including deliberate introduction of recombination centers to stabilize response time at a required level and by reducing the lifetime in short photoconductors using contact phenomena. Further work is necessary to understand the origin and properties of the deep centers in GaN.

For several applications, such as furnace plot flame detection, missile plume measurements, and astronomy, it is highly desirable to move the long wavelength cutoff below 300 nm to avoid interference from solar radiation. This is the motivation for fabrication and characterization of intrinsic photoconductors using $Al_xGa_{1-x}N$ epitaxial layers with x values ranging from 0 to 1 [with cutoff wavelengths from 200 nm (AlN) to 365 nm (GaN)] [44–46]. Figure 11 shows the normalized photoresponse from $Al_xGa_{1-x}N$ photoconductors with x = 1, 0.75 and 0.63. The Al composition tunes the cutoff wavelength, which varies from about 200 nm for AlN to 240 nm for $Al_{0.63}Ga_{0.37}N$. The effective carrier lifetime obtained from the frequency dependent photoresponse measurements were 35 ms, 25 ms and 17.5 ms for x = 1, 0.75, and 0.63, respectively.

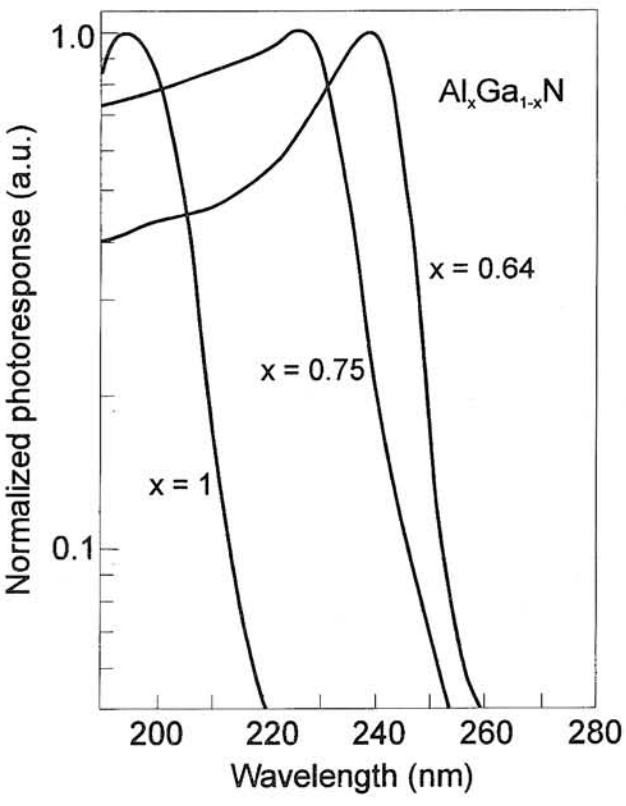

Fig. 11. Normalized photoresponse of $Al_xGa_{1-x}N$ photoconductors with x = 1, 0.75 and 0.63. The corresponding cutoff wavelengths are 200nm, 230 nm and 240 nm (after Ref. 46).

6.2. Photovoltaic detectors

6.2.1. Schottky barrier photodiodes

The first Schottky GaN barriers were reported over 20 years ago [47]. However due to a fabrication procedure, that was not well controlled, an anomalous behaviour of electrical properties of these Zn/GaN Schottky barriers has been observed.

More recently Khan et al. [48] have reported the fabrication and characterization of Schottky barrier photodiodes on p-type GaN layers. As-grown 2-μm-thick material (grown over basal plane sapphire using MOCVD) was a n-type conductivity with residual carrier concentration of 10^{17} cm^3 and a room temperature mobility of about 400 cm^2/Vs. Post-growth, p-type conductivity was enhanced using a 20 min 650°C N_2 ambient anneal. After this process, the hole concentration was about $7x10^{17}$ cm^3. Subsequent to growth, doughnut-shaped Cr/Au (2000-Å-thick) ohmic contacts were deposited using standard photolithographic techniques. The inside diameters for the doughnuts were ranged from 200 μm to 1 mm. For improving the contact resistivities, the ohmic contacts were annealed in flowing forming gas at 350 Å for 1 min. As a Schottky barrier 1500-Å-thick Ti/Au metals were deposited. The estimated responsivity of these Schottky barriers were 0.13 A/W at wavelenght 320 nm for a normalized area of 1 mm^2. The response time of detectors is limited by the resistance capacitance (RC) time constant of the measured circuit and was around 1 μs.

It should be noticed that much information concerning GaN Schottky barriers is under discussion [49]. The barrier height depends on a procedure used for diode fabrication (surface states and process-induced defects). Figure 12 shows the barrier height (determined from I–V–T characteristics) of several metals on n-type GaN plotted

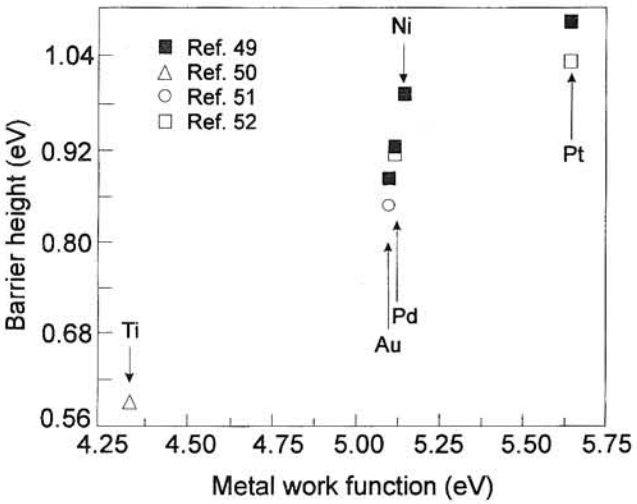

Fig. 12. Relation of barrier height to metal work-function for n-type GaN (after Ref. 49).

as a function of their metal work function. Binari et al. [50] reported a barrier height Φ_b of 0.58 eV for Ti/n-GaN, however another results show that ligtly rectifying, which indicates very low Φ_b. As seen in this figure, a monotonic increase in Φ_b is observed as metal workfunction increases. However, the increase does not scale with the workfunction as expected from the relation, $q\Phi_b = q\Phi_m - q\chi$, where Φ_b and χ are the metal workfunction and the semiconductor electron affinity, respectively. The electron affinity of GaN has been determined to be $\approx$ 4.1 eV. This indicate that the Schottky barrier height on n-type GaN is also influenced by other factors besides metal work-function.

6.2.2. p-n junction photodiodes

The first information about p-n junction GaN photovoltaic detectors is included in Ref. 35. Next, Chen et al. [53] have studied two detector structures grown by low pressure MOCVD, one n-on-p and the other p-on-n. The p-on-n sample consisted of the deposition over basal plane sapphire of a 1 μm thick unintentionally doped n-GaN layer followed by a 0.5 μm thick Mg-doped p-GaN layer. Similarly, the n-on-p structure consisted of a 1 μm p-GaN layer followed by a 0.5 μm n-GaN layer. Large area mesa structures were defined using reactive ion etching (Fig. 13). Ohmic contacts were formed using sputtered W for

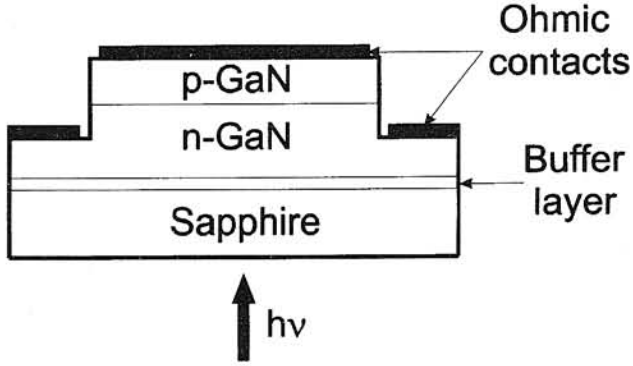

Fig. 13. GaN p-n junction structures (after 35).

n- and e-beam evaporated Ni/Au bilayer for the p-contacts. The spectral responsivity data are plotted in Fig. 14. The maximum responsivity (0.09 A/W) is comparable to that of a UV-enhanced Si detector.

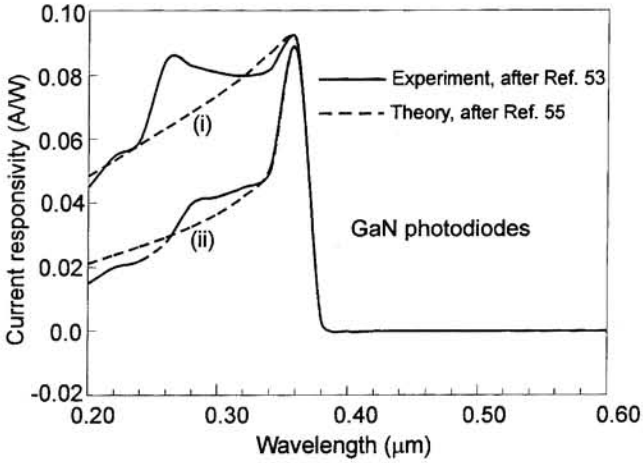

Fig. 14. Spectral current responsivity of GaN photodiodes: (i) UV illumination from n-type side, (ii) UV illumination from p-type side. The experimentally measured curves (solid lines) are taken from Ref. 53. The theoretical curves (solid curves) adjusted to experimental data (dashed curves) are calculated assuming: L_h = 0.49 μm, s_1 = 0 and L_e = 1.8 μm, s_1 = 5x10^4 cm/s for photodiode structures illuminated from n-type and p-type layers, respectively, with the reflection coefficient r = 0.12 (after Ref. 55).

One of the most important parameters of photodiodes is the diffusion length of minority carriers. Zhang et al. [54] have studied photovoltaic effect of device structure with p-n junction connected

back-to-back with a Schottky barrier. They also estimated the diffusion length of holes in the n-type GaN layer on 0.1 μm. It is rather very short minority carrier diffusion length. Recently, for the first time, the minority carrier diffusion lengths in n-on-p and p-on-n GaN photodiodes have been estimated by Małachowski and Rogalski [55]. The estimation procedure has consisted in adjustment of theoretically predicted spectral responsivity of GaN photodiodes to experimentally measured responsivity presented by Q. Chen et al. [53] (see Fig. 14). It has been found that due to the strong absorption of UV radiation in GaN material, the depleted region and the backside layer of the p-n junction have a minor contribution to the quantum efficiency. The minority carrier diffusion length of 1.8 μm and 0.49 μm have been estimated for electrons in the p-type region and holes in n-type region, respectively.

More sophisticated structures are also used for the detection of UV radiation. Recently Khan et al. [56, 57] have reported the GaN/AlGaN heterostructure field effect transistors (HFETs) as gated visible blind photodetectors. The maximum responsivity of 3000 Å/W was achieved at a gate voltage of about 1 V. The spectral responsivity falls sharply by two orders of magnitude for wavelengths larger than 365 nm, which demonstrates the visible blind operation of gated photodetector.

7. Other UV detectors

A straightforward way to make a highly selective (blindless) UV detector is to use a wide-bandgap semiconductor. Schottky barrier UV detectors have been fabricated using different semiconductors, e.g. ZnO [58], GaAsP [59–61], and diamond [62]. Constant et al. [63] have presented GaAs photoconductive detectors with static responsivity values of 10^7–10^8 A/W in UV spectral range. The principal advantage of GaAs detectors lies in the high crystalline quality of the material and its weell-known processing methods. Misra et al. [64] have presented preliminary results concerning fabrication and characterization of BNP photoconductive detectors. This alloy system is an attractive material for UV application because its bandgap can be tuned in the UV region (between 200 nm and 400 nm). Recently, for the first time, the dramatic improvement in diamond photoconductive characteristics (10^6 higher response to 200 nm than visible wavelengths, dark current < 0.1 nA) has been achieved following methane-air treatment of the polycrystalline material [65].

Conclusions

Currently, the old detection techniques used in UV technology (photographic films, detectors based on gas photoionization, and photoemissive detectors) are replaced by semiconductor photon detectors where higher sensitivity, more quantitatively accurate photometric information, or more immediate data availability is required. The semiconductor detectors offer small size, ruggedness, and ease of use. Expansion of the semiconductor industry and the continuing emphasis on the development of low-light-level imaging systems for military and civilian surveillance applications ensure the dominant position of these detectors in the near future. Manufactured using proven wafer-scale silicon or III-V processing techniques, they are inherently cheaper and provide high quantum efficiency. However, Si photodetectors require bulky band filters to block the visible solar radiation background and are intolerant of elevated temperatures and caustic environments. With the use of wide bandgap semiconductors (like GaN or diamond), the need for these filters will be largely eliminated simplifying the design of the spectroscopic monitoring equipment. Moreover, these devices are potentially free from the mentioned shortcomings; they are capable to operate at high temperatures and hostile environments.

Interest in new generation of wide bandgap semiconductor detectors stems in part from the fact that the earth's atmosphere is opaque at wavelength below 300 nm. To take advantage of this optical window, earth to space communication will need detectors that are UV sensitive but blind to the ambient visible radiation. Another area where these detectors can find applications is in the combustion monitoring of gases where UV emission is a normal byproduct.

Semiconductor diamond is of considerable interest for UV detectors from a basic physical properties. Unfortunately, diamond of a good-enough quality is not readily available, and approp-

riate technology is far from being mature. However, recent progress in diamond thin films technology is promising for future applications.

Unlike SiC, which is another wide bandgap semiconductor with demonstrated n- and p-type doping and excellent power device performance, one notable advantage of III-V nitrides is that they form direct bandgap heterostructures, have better ohmic contacts and heterostructures. Because of this, it is anticipated that III-V nitrides may eventually prove to be more promising than SiC for optoelectronic devices.

The future direction in research and development of GaN-based UV detectors (mainly photodiodes) judges from the remarkable progress in its performance attained over the last few years. A late news paper at International Electron Device Meeting announces the first observation of stimulated emission from a current injected InGaN/AlGaN double-heterostructure diode [66, 67]. The major obstacle prohibiting the sort of improvement needed is the large concentration of defects, although some attribute some of the shortcoming to processing related problems. Large concentration of defects (10^7–10^{10} cm^{-2}) in GaN structures manifest themselves as short carrier lifetimes and reduced photoluminescence intensity. Further progress will more likely be due to the use of better matched substrates. A great deal of effort is presently being expended in laboratories everywhere to search for a better substrate ($LiGaO_2$, $LiAlO_2$, and $MgAl_2O_4$ appear to be promising candidates) or compliant base to decrease the defect generation, and thus increase quantum efficiency and photoconductive gain of detectors [68].

References

1. G.R. Carruthers: *Ultraviolet and X-ray detectors. In: Electro-Optics Handbook,* Chapter 15, ed. by R. W. Waynant and M.N. Ediger, McGraw-Hill, New York 1994.
2. J.G. Timothy and R. P. Madden: *Photon detectors for the ultraviolet and X-ray region.* In: Handbook on Synchrotron Radiation, p. 315, ed. by E. E. Koch, North-Holland, Amsterdam 1983.
3. M.J. Eccles, M. E. Sim, and K. P. Tritton: *Low Light Level Detectors in Astronomy.* Cambridge University Press, Cambridge 1983.
4. J.G. Timothy: *Optical detectors for spectroscopy.* Publications of the Astronomical Society of the Pacific, **95** (1983) 810.
5. J.R. Janesick, T. Elliott, S. Collins, H. Marsh, M. Blouke and M. Freeman: *The future scientific CCD.* Proc. SPIE **501** (1984) 2.
6. B.Y. Welsh and M. Kaplan: *NASAs ultraviolet astrophysics branch: the next decade.* Proc. SPIE **1743** (1992) 452.
7. C.L. Joseph: *UV image sensors and associated technologies.* Wisconsin Astrophysics **562** (1995) 1.
8. M.P. Ulmer, M. Razeghi and E. Bigan: *Ultra-violet detectors for astrophysics, present and future.* Proc. SPIE **2397**, (1995) 210.
9. J.R. Janesick, D. Campbell, T. Elliott and T. Daud: *Flash technology for charge-coupled--device imaging.* Opt. Eng. **26** (1987) 825.
10. R.A. Stern, R.C. Catura, R. Kimble, A.F. Davidsen, M. Winzenread, M.M. Blouke, R. Hayes, D.M. Walton and J.L. Culhane: *Ultraviolet and extreme ultraviolet response of charge-coupled-device detectors.* Opt. Eng. **26** (1987) 875.
11. J.R. Janesick, T. Elliott, G. Fraschetti, S. Collins, M. Blouke and B. Corrie: *Charge-coupled device pinning technologies.* Proc. SPIE **1071** (1989) 153.
12. G.M. Williams and M. M. Blouke: *How to capture low-light-level images without intensifiers.* Laser Focus World, (September 1995) 129.
13. M. Razeghi and A. Rogalski: *Semiconductor ultraviolet detectors.* J. Appl. Phys. **79** (1996) 7433.
14. D.H. Seib and L.W. Aukerman: *Photodetectors for the 0.1 to 1.0 μm spectral region. In: Advances in* Electronics and Electron Physics, **34**, p. 95, ed. by L. Morton, Academic Press, New York 1973.
15. S. Strite and H. Morkoc: *GaN, AlN, and InN: A review.* J. Vac. Sci. Technol. **B10** (1992) 1237.

16. H. Morkoc, S. Strire, G.B. Gao, M.E. Lin, B. Sverdlov and M. Burns: *Large-band-gap SiC, III-V nitride, and II-VI ZnSe-based semiconductor device technologies.* J. Appl. Phys. **76** (1994) 1363.
17. M. Marchywka, S.C. Binari, P.E. Pehrsson, D. Moses: *Recent results in diamond UV detector research.* Proc. SPIE **2282** (1994) 20.
18. Y. Talmi and R.W. Simpson: *Self-scanned photodiode array: a multichannel spectrometric detector.* Appl. Opt. **19** (1980) 1401.
19. T.E. Hansen: *Silicon UV-photodiodes using natural inversion layers.* Phys. Scr. **18** (1978) 471.
20. R.Korde and J. Geist: *Quantum efficiency stability of silicon photodiodes.* Appl. Opt. **26** (1987) 5284.
21. L.R. Canfield, R. Vest, T. N. Woods and R. Korde: *Silicon photodiodes with integrated thin film filters for selective bandpasses in the extreme ultraviolet.* Proc. SPIE **2282** (1994) 31.
22. R. Korde, L.R. Canfield and B. Wallis: *Stable, high quantum efficiency silicon photodiodes for vacuum-UV applications.* Proc. SPIE **932**, (1988) 153.
23. R. Korde and J. Geist: *Stable, high quantum efficiency, UV-enhanced silicon photodiodes by arsenic diffusion.* Soild-State Electronics **30** (1987) 89.
24. L.R. Canfield, J. Kerner and R. Korde: *Stability and quantum efficiency performance of silicon photodiode detectors in the far ultraviolet.* Appl. Opt. **28** (1989) 3940.
25. S.G. Chamberlain: *New profiled silicon photodetector for improved short-wavelength quantum efficiency.* J. Appl. Phys. **50** (1979) 7228.
26. H. Ouchi, T. Mukai, T. Kamei, and M. Okamura: *Silicon p-n junction photodiodes sensitive to ultraviolet radiation.* IEEE Trans. Electron Devices **ED-26** (1979) 1965.
27. R.B. Campbell and H. Chang: *Detection of ultraviolet radiation using silicon carbide p-n junctions.* Solid-State Electronics **10** (1967) 949.
28. P. Glasow, G. Ziegler, W. Suttrop, G. Pensl and R. Helbig: *SiC-UV-photodetectors".* Proc. SPIE **868** (1987) 40.
29. D.M. Brown, E.T. Downey, M. Ghezzo, J.W. Kretchmer, R.J. Saia, Y.S. Liu, J.A. Edmond, G. Gati, J.M. Pimbley and W.E. Schneider: *Silicon carbide UV photodiodes.* IEEE Trans. Electron Devices **40** (1993) 325.
30. J.A. Edmond, H.S. Kong and C.H. Carter Jr.: *Blue LEDs, UV photodiodes and high-temperature rectifiers in 6H-SiC.* Physics B **185** (1993) 453.
31. D. Caputo, G. de Cesare, F. Irrera and F. Palma: *Solar-blind UV photodetectors for large area applications.* IEEE Trans. Electron Devices **43** (1996) 1351.
32. C. Fröjdh, G. Thungström, H.E. Nilsson and C.S. Petersson: *UV-sensitive photodetectors based on metal-semiconductor contacts on 6H-SiC.* Physica Scripta **T54** (1994) 169.
33. C. Fröjdh, G. Thungström, H.E. Nilsson and C.S. Petersson: *UV-sensitive metal-semiconductor photodiodes on 6H-SiC.* Mat. Res. Soc. Symp. Proc. **339** (1994) p. 215.
34. I. Akasaki and H. Amano: *Widegap column-III nitride semiconductors for UV/blue light emitting devices.* J. Electrochem. Soc. **141** (1994) 2266.
35. M.A. Khan, Q. Chen, C.J. Sun, M.S. Shur, M.F. Macmillan, R.P. Devaty and J. Choyke: *Optoelectronic devices based on GaN, AlGaN, InGaN homo-heterojunctions and supperlattices.* Proc. SPIE **2397** (1995) 283.
36. M.A. Khan, J.N. Kuznia, D.T. Olson, J.M. Van Hove, M. Blasingame and L.F. Reitz: *High--responsivity photoconductive ultraviolet sensors based on insulating single-crystal GaN epilayers.* Appl. Phys. Lett. **60** (1992) 2917.
37. Z. C. Huang, J. C. Chen, D. B. Mott and P. K. Shu: *High performance GaN linear array",* Electronics Letters **32** (1996) 14.
38. C.H. Qiu, C. Hoggatt, W. Melton, M.W. Leksono and J.I. Pankove: *Study of deffect states in GaN films by photoconductivity measurements.* Appl. Phys. Lett. **66** (1995) 2712.
39. K.S. Stevens, M. Kinniburgh and R. Beresford: *Photoconductive ultraviolet sensor using Mg-doped GaN on Si(111).* Appl. Phys. Lett. **66** (1995) 3518.
40. P. Kung, X. Zhang, D. Walker, A. Saxler, J. Piotrowski, A. Rogalski and M. Razeghi: *Kinetics of photoconductivity in n-type GaN photodetector.* Appl. Phys. Lett. **67** (1995) 3792.
41. F. Binet, J.Y. Duboz, E. Rosencher, F. Scholz and V. Härle: *Mechanisms of recombination in GaN photodetectors.* Appl. Phys. Lett. **69** (1996) 1202.
42. C.H. Qiu, W. Melton, M. W. Leksono, J.L. Pankove, B.P. Keller and S.P. BenBaars: *Pho-*

tocurrent decay in n-type GaN thin films. Appl. Phys. Lett. **69** (1996) 1282.

43. B. Goldenberg, J.D. Zook, and R.J. Ulmer: *Fabrication and performance of GaN detectors.* Topical Workshop on III-V Nitrides Proc., Nagoya, Japan, (1995).
44. D. Walker, X. Zhang, P. Kung, A. Saxler, S. Javadpour, J. Xu and M. Razeghi: *AlGaN ultraviolet photoconductors grown on sapphire.* Appl. Phys. Lett. **68** (1996) 2100.
45. B.W. Lim, Q.C. Chen, J.Y. Yang and M. Asif Khan: *High responsivity intrinsic photoconductors based on $Al_xGa_{1-x}N$.* Appl. Phys. Lett. **68** (1996) 3761.
46. X. Zhang, A. Saxler, P. Kung, D. Walker and M. Razeghi: *Intrinsic $Al_xGa_{1-x}N$, AlN photoconductors with cut-off wavelengths from 240 to 200 nm.* Appl. Phys. Lett. (to be published).
47. Y. Morimoto and S. Ushio: *Anomalous behaviour in GaN-Zn junctions.* Jap. J. Appl. Phys. **13** (1974) 365.
48. M.A. Khan, J.N. Kuznia, D.T. Olson, M. Blasingame and A.R. Bhattarai: *Schottky barrier photoconductor based on Mg-doped p-type GaN films.* Appl. Phys. Lett. **63** (1993) 2455.
49. A.C. Schmitz, A.T. Ping, M.A. Khan, Q. Chen, J. W. Yang and I. Adesida: *Schottky barrier properties of various metals on n-type GaN.* Semicond. Sci. Technol. **11** (1996) 1464.
50. S.C. Binari, H.B. Dietrich, G. Kelner, L.B. Rowland, K. Doverspike and D.K. Gaskill: *Electrical characterisation of Ti Schottky barriers on n-type GaN.* Electronics Letters **30** (1994) 909.
51. P. Hacke, T. Detchprohm, K. Hiramatsu and N. Sawaki: *Schottky barrier on n-type GaN grown by hydride vapor phase epitaxy.* Appl. Phys. Lett. **63** (1993) 2676.
52. J.D. Guo, M.S. Feng, R.J. Guo, F.M. Pan and C.Y. Chang: *Study of Schottky barrier on n-type GaN grown by low-pressure metalorganic chemical vapor deposition.* Appl. Phys. Lett. **67** (1995) 2657.
53. Q. Chen, M.A. Khan, C.J. Sun and J.W. Yang: *Visible-blind ultraviolet photodetectors based on GaN p-n junctions.* Electronics Letters **31** (1995) 1781.
54. X. Zhang, P. Kung, D. Walker, J. Piotrowski, A. Rogalski, A. Saxler and M. Razeghi: *Photovoltaic effects in GaN structures with p-n junctions.* Appl. Phys. Lett. **67** (1995) 2028.
55. M.J. Małachowski and A. Rogalski: *GaN ultraviolet photodiodes – performance modeling.* J. Technical Physics (to be published).
56. M.A. Khan, M.S. Shur, Q. Chen, J.N. Kuznia and C.J. Sun: *Gated photodetector based on GaN/AlGaN heterostructure field effect transistor.* Electronics Letters **31** (1995) 398.
57. M.S. Shur and M.A. Khan: *Optoelectronic GaN-based field effect transistors.* Proc. SPIE **2397** (1995) 294.
58. H. Fabricius, T. Skettrup and P. Bisgaard: *Ultraviolet detectors in thin sputtered ZnO films.* Appl. Opt. **25** (1986) 2764.
59. M. Krumrey, E. Tegler, J. Barth, M. Krisch, F. Schafers and R. Wolf: *Schottky type photodiodes as detectors in the VUV and soft x-ray range.* Appl. Opt. **27** (1988) 4336.
60. E. Tegeler and M. Krumrey: *Stability of semiconductor photodiodes as VUV detectors",* Nucl. Instr. and Meth. **A282** (1989) 701.
61. A.D. Wilson and H. Lyall: *Design of an ultraviolet radiometer. 1: Detector electrical characteristics.* Appl. Opt. **25** (1986) 4530; *Design of an ultraviolet radiometer. 2: Detector optical characteristics.* Appl. Opt. **25** (1988) 2540.
62. G. Zhao, T. Stacy, E.M. Charlson, E.J. Charlson, M. Hajsaid, R. Roychoudhury, A.H. Khan, J.M. Meese, Z. He and M. Prelas: *Photoresponse study of polycrystalline diamond thin films Schottky diodes.* Mat. Res. Soc. Symp. Proc. **339** (1994) 191.
63. M. Constant, D. Loridant, J. C. Camart, S. Meziere, L. Boussekey and M. Chive: *New capabilities of GaAs detectors for UV applications.* Proc. SPIE **2367** (1995) 229.
64. M. Misra, C. Zhou, P.B. Bennett, M.R. Squillants and F. Ahmad: *Novel material for visible-blind ultraviolet detectors.* Proc. SPIE **2282** (1994) 49.
65. R. D. McKeag, S. S. M. Chan, and R. B. Jackman: *Polycrystalline diamond photoconductive device with high UV-visible discrimination.* Appl. Phys. Lett. **67** (1995) 2117.
66. Compound Semiconductors, (Nov/Dec 1995), 8.
67. S. Nakamura, M. Senoh, S. Nagahama, N. Iwasa, T. Yamada, T. Matsushita, H. Kiyoku and Y. Sugimoto: *InGaN-based multi-quantum-well-structure laser diodes.* Jpn. J. Appl. Phys. **35**, (1996) 74.
68. Compound Semiconductors, (Nov/Dec 1995), 9.